An Alpha Tubulin Mutation Suppresses Nuclear Migration Mutations in *Aspergillus nidulans*

Debra Aker Willins, Xin Xiang and N. Ronald Morris

Department of Pharmacology, UMDNJ-Robert Wood Johnson Medical School, Piscataway, NJ 08854-5635

Manuscript received April 19, 1995
Accepted for publication September 12, 1995

ABSTRACT

Microtubules and cytoplasmic dynein, a microtubule-dependent motor, are required for nuclei to move along the hyphae of filamentous fungi. Nuclear migration in *Aspergillus nidulans* is blocked by heat-sensitive (hs^-) mutations in the *nudA* gene, which encodes dynein heavy chain, and the *nudF* gene, which encodes a G protein β-subunit-like protein. Hs^- mutations in the *nudC* and *nudG* genes also prevent nuclear migration. We have isolated extragenic suppressor mutations that reverse the hs^- phenotypes caused by these mutations. Here we show that one *nudF* suppressor also suppresses hs^- mutations in *nudA*, *nudC*, and *nudG* and deletions in *nudA* and *nudF*. This suppressor mutation is in the *tubA* alpha tubulin gene, and its characteristics suggest that it destabilizes microtubules. The mutation alters microtubule staining and confers sensitivity to cold and benomyl, two treatments that destabilize microtubules. Treatment with low concentrations of benomyl also suppresses the hs^- *nudA*, *nudC*, *nudF*, and *nudG* mutations and the *nudA* and *nudF* deletions. Suppression of the hs^- *nudA* mutation and the *nudA* deletion is especially interesting because these strains lack active dynein heavy chain. Together, these results suggest that microtubule destabilization allows nuclei to migrate even in the absence of cytoplasmic dynein motor function.

NUCLEAR migration is ubiquitous among eukaryotes, with roles in development and other biological phenomena. Nuclear movement brings together parental nuclei before fertilization in yeast and in sea urchin eggs (SCHATTEN 1982; ROSE 1991). In Drosophila embryos, nuclei move from random positions to a single layer under the cortex just prior to cellularization (ZALOKAR and ERK 1976). Nuclear position determines the location of the mitotic cleavage in sea urchin and mouse embryos and, therefore, whether daughter cells are equal or unequal in size (DAN 1979; REEVE and KELLY 1983). In *Saccharomyces cerevisiae,* the nucleus moves toward the bud before mitosis, allowing proper segregation of the daughter nucleus into the bud (HUFFAKER *et al.* 1988). The position of the nucleus in neuroepithelial cells may determine their shape and their ability to form a folding cell layer (SMITH and SCHOENWOLF 1988). Finally, nuclear migration may be required for cell movement during brain development (BOOK *et al.* 1991) and tumor cell metastasis (KLOMINEK *et al.* 1991). Despite its importance, the details of nuclear migration are not well known. We anticipate that many of the proteins involved in nuclear migration will be conserved between *Aspergillus nidulans* and other eukaryotes.

In filamentous fungi, spore germination is accompanied by multiple divisions of the nucleus and migration of the daughter nuclei into the growing hyphae. Microtubules and the microtubule motor cytoplasmic dynein are required for distribution of nuclei along the multinucleate hyphae of *A. nidulans* and *Neurospora crassa* (OAKLEY and MORRIS 1980; PLAMANN *et al.* 1994; XIANG *et al.* 1994). Heat-sensitive mutations that prevent nuclear distribution in *A. nidulans,* designated *nud* mutations, were isolated by MORRIS (1976). *nud* mutants grown at the restrictive temperature show normal germination and nuclear division, but the nuclei remain at their origin in the spore body. At the restrictive temperature, *nud* mutants grow poorly, are defective in asexual spore development, and show excessive hyphal branching. Finally, the *nud* defect is independent of nuclear division because *A. nidulans* mutants blocked in nuclear division still demonstrate nuclear migration (OAKLEY and MORRIS 1980; OSMANI *et al.* 1990). PLAMANN *et al.* (1994) characterized similar mutations in *N. crassa* affecting nuclear migration, hyphal branching, and sexual reproduction, designated *ropy* mutations for their morphological phenotype.

Four *nud* genes of *A. nidulans* (*nudA, nudC, nudF,* and *nudG*) have been identified. Cloning of *nudG* is in progress (S. BECKWITH and N. R. MORRIS, unpublished results), and the other three genes have been cloned. *nudA* encodes the heavy chain of cytoplasmic dynein (XIANG *et al.* 1994), an ATP-dependent minus-end directed microtubule motor (VALLEE 1993). Deletion and disruption studies show that the heavy chain is essential for nuclear migration in *A. nidulans* and *S. cerevisiae* (ESHEL *et al.* 1993; LI *et al.* 1993; XIANG *et al.* 1995b).

Corresponding author: N. Ronald Morris, Department of Pharmacology, UMDNJ-Robert Wood Johnson Medical School, 675 Hoes Lane, Piscataway, NJ 08854-5635. E-mail: rmorris@biovax.rutgers.edu

nudC encodes an evolutionarily conserved 22 kDa protein, and a mutation in *nudC* affects the level of the *nudF* product (OSMANI *et al.* 1990; XIANG *et al.* 1995a). The *nudF* gene was isolated as an extra-copy suppressor of *nudC* that also complemented two hs$^-$ *nudF* mutations (XIANG *et al.* 1995a). *nudF* encodes a protein with WD repeats also found in the beta subunit of transducin, a heterotrimeric G protein involved in signal transduction. Among the proteins in the WD-repeat family, the *nudF* product is most similar to human LIS-1, with 42% identity overall (XIANG *et al.* 1995a). Heterozygous LIS-1 deletions cause Miller-Dieker lissencephaly, a disease characterized by defective neuronal cell migration and abnormal brain development (BARTH 1987; REINER *et al.* 1993).

Eight *ropy* genes that mediate nuclear migration in *N. crassa* have been identified, and three have been cloned (*ro-1, ro-3,* and *ro-4*). The *ro-1* gene encodes cytoplasmic dynein heavy chain (PLAMANN *et al.* 1994). The *ro-3* gene encodes a protein homologous to p150^{Glued} (cited in PLAMANN *et al.* 1994). The p150^{Glued} protein is a component of the dynactin complex, which participates with dynein in moving organelles (VALLEE 1993; SCHROER 1994). The *ro-4* gene encodes the actin-related protein Arp1 (centractin), a major component of the dynactin complex (PLAMANN *et al.* 1994; ROBB *et al.* 1995).

To identify additional genes affecting nuclear migration in *A. nidulans* or to uncover interactions among known genes, we isolated extragenic suppressors of *nudF*. One of these has a mutation in *tubA* alpha tubulin that partially suppresses *nudF* and the other *nud* mutations, apparently by destabilizing microtubules.

MATERIALS AND METHODS

Strains and growth conditions: Table 1 lists the *A. nidulans* strains used. Solid medium was YAG (0.5% yeast extract, 2% glucose, trace elements, 2% agar) (KÄFER 1977). Liquid medium was YAG without agar. YAG was supplemented with 5 mM uridine and 10 mM uracil for growth of *pyrG89* strains and 6.6 μM riboflavin for *riboA1* strains (KÄFER 1977). Growth on YAG supplemented with 0.7 M KCl increased the yield of conidia (asexual spores) from *nud* mutants, but all colony growth experiments were done in the absence of KCl. Benomyl (50% benomyl from Bonide Chemical Co., Yorkville, NY, or 98% benomyl from DuPont) was added to medium from a 1 mg/ml stock in 95% ethanol. Growth on solid medium was generally for 6–7 days at 18°, 3 days at 32°, and 2 days at 43°.

General *A. nidulans* techniques: *A. nidulans* techniques were as previously described (PONTECORVO *et al.* 1953; CLUTTERBUCK 1974; KÄFER 1977). Standard molecular biology techniques were used for construction and purification of plasmids (SAMBROOK *et al.* 1989). *A. nidulans* genomic DNA was prepared by a modification of the procedure of OAKLEY *et al.* (1987b). Pulverized freeze-dried hyphal material was extracted with 50 mM EDTA, pH 8, 0.2% SDS, 0.1% (v/v) DEPC at 65° for 20 min and centrifuged at low speed to remove cell debris. The extract was mixed with one-half volume of 5 M potassium acetate, incubated on ice for 15 min, and centrifuged, and the nucleic acid in the supernatant was precipitated with isopropanol. The resulting nucleic acid was purified further by LiCl-ethanol precipitation. Southern blotting was performed with Zeta-Probe GT Blotting Membrane (Bio-Rad) and probe labeled by the Random Primers DNA Labeling System (Life Technologies), both according to the manufacturers' instructions.

Mutagenesis: A suspension of 10^8 conidia (asexual spores) in 10 ml sterile water was irradiated with UV light at a distance of 23 cm for 15 sec with gentle agitation. Spores were from strain XX20 (*nudF6, pyrG89*). At the dosage used, 8000 erg/sec/cm^2, about 15% of the mutagenized spores were viable. To recover hs$^+$ revertants, mutagenized spores were plated at 43°. An overlay of agar was added after 1 day to reduce background hs$^-$ growth (hs$^+$ revertants grow through the overlay but hs$^-$ cells do not). About 1000 hs$^+$ revertants remained after rescreening.

Construction of pDW1: The *tubA* plasmid pDP485, which contains a 4.9-kb *Sac*I genomic DNA fragment cloned into pUC19 (DOSHI *et al.* 1991), was cut with *Bam*HI and *Dra*I. The 2.4-kb *Bam*HI-*Bam*HI fragment carrying *tubA* was inserted into the *Bam*HI site of pUC19 to generate pDW1. This fragment includes the sequence from 20 bp upstream of the *tubA* ATG start codon to about 600 bp downstream of the stop codon. The *A. nidulans* DNA insert in pDW1 is not likely to contain the *tubA* promoter and does not contain any long open reading frames other than *tubA*. Linearized pDW1 was prepared by digestion with *Aat*II, *Xba*I, and *Dra*I (which cut only in the vector), followed by alkaline phosphatase treatment and purification by agarose gel electrophoresis.

***nudF* and *nudA* deletion strains:** The Δ*nudF* strain ΔF54 was constructed by using the plasmid pXX10 to replace the wild-type genomic *nudF* sequence with the *N. crassa pyr4* marker gene (Figure 1A). The plasmid pXX10 contains *pyr4* with *nudF* flanking sequences but lacks the *nudF* coding sequence (except for 12 N-terminal amino acids). It was constructed from four DNA fragments, as follows. For the 5′ flanking sequence of *nudF,* the 3.9-kb *Eco*RI fragment of the genomic clone λ3 (XIANG *et al.* 1995a) was subcloned into pBluescript KS(+) and a 2.1-kb *Hin*dIII-*Xba*I fragment (fragment A) was excised. For the 3′ flanking sequence of *nudF,* the 3.8-kb *Eco*RI-*Eco*RI* fragment of λ5 (XIANG *et al.* 1995a) was cloned into pBluescript KS(+), a 1.6-kb *Hin*dIII fragment was excised and subcloned into pBluescript KS(+), and the *Hin*dIII fragment was excised as a *Cla*I-*Eco*RI fragment (fragment B). The orientation of the insert in the *Hin*dIII subclone (verified by sequencing) is such that the *Cla*I site is a few nucleotides away from the *Hin*dIII site in the 3′ untranslated region of *nudF*. For the marker gene, a 2.1-kb *Pst*I-*Sma*I *pyr4* fragment derived from a 2.1-kb *Eco*RI fragment (O'CONNELL *et al.* 1993) was cloned into pBluescript KS(+). *Pyr4* was excised as a *Xba*I-*Cla*I fragment (fragment C), which complements the *A. nidulans pyrG89* mutation. To make plasmid pXX10, pBluescript KS(+) cut with *Hin*dIII and *Eco*RI was ligated to a mixture of fragments A, B, and C. Sequencing analysis confirmed that the pXX10 clone was constructed correctly except for a single base mutation destroying the *Xba*I site. *A. nidulans* strain GR5 was transformed with pXX10 DNA, which was linearized by digestion with *Not*I (which cuts in the vector). Transformants that had a *nud* phenotype were analyzed by Southern blotting to identify ones with pXX10 DNA integrated only at the *nudF* locus (*e.g.,* strain ΔF54) (Figure 1B). The Δ*nudF* strain ΔF54 exhibited a nuclear migration defect (Figure 1C). In Δ*nudA* strain XX60, the four putative ATP binding sites of dynein heavy chain (amino acids 1929–2965) were deleted and replaced with the *A. nidulans pyrG* marker (XIANG *et al.* 1995b). The Δ*nudA* deletion also

TABLE 1

***A. nidulans* strains**

Strain	Genotype	Source
SJ002	*pyrG89*	S. JAMES
FGSC154	*adE20, biA1, wA2, cnxE16, sC12, methG1, nicA2, lacA1, choA1, chaA1*	Fungal Genetics Stock Center
GR5	*pyrG89, wA2, pyroA4*	G. MAY
R21	*pabaA1, yA2*	C. F. ROBERTS
R153	*wA3, pyroA4*	C. F. ROBERTS
XX20	*nudF6, pyrG89*	XIANG *et al.* (1995a)
DW7	*wA3, nudF6, pyroA4*	This work, from XX20 × R153
DW15	*pyrG89, nudF6, tubA22 (snfA890)*	This work, from UV mut. of XX20
DW16	*wA3, pyroA4, nudF6, tubA22 (snfA890)*	This work, from DW15 × R153
DW17	*wA3, pyroA4, tubA22 (snfA890)*	This work, from DW15 × R153
DW26	*wA3, pyroA4, pyrG89, nudF6, tubA22 (snfA890)*	This work, from DW15 × R153
DW27	*wA3, pyrG89, tubA22 (snfA890)*	This work, from DW15 × R153
LO12	*AcrA1, sD85, tubA1 (possibly other markers)*	C.E. OAKLEY and B. R. OAKLEY
LO14	*tubA1, suA1-adE20, proA1, pabaA1, yA2, adE20, AcrA1*	GAMBINO *et al.* (1984)
DW29	*fwA1, tubA1, pyrG89, pabaA1, (AcrA1?)*	This work, progeny of LO12
XX3	*nudA1, pyrG89, chaA1*	XIANG *et al.* (1994)
YH1	*nudC3, riboA1, yA2*	Y. CHIU, N. R. MORRIS lab
XX21	*nudF7, pyrG89, yA2*	XIANG *et al.* (1995a)
SB05.10	*nudG8, yA2, pabaA1*	S. BECKWITH, N. R. MORRIS lab
ΔF54	Δ*nudF::pyr4*$^+$, *pyrG89, wA2, pyroA4*	This work
XX60	Δ*nudA::pyrG*$^+$ (partial deletion), *pyrG89*	XIANG *et al.* (1995b)
DW30	*nudA1, tubA22 (snfA890), pyrG89*	This work, from DW17 × XX3
DW31	*nudA1, tubA22 (snfA890), pyrG89, wA3*	This work, from DW17 × XX3
DW32	*nudC3, tubA22 (snfA890), yA2, riboA1*	This work, from DW17 × YH1
DW33	*nudF7, tubA22 (snfA890), pyrG89, yA2*	This work, from DW17 × XX21
DW34	*nudG8, tubA22 (snfA890), yA2, pabaA1*	This work, from DW17 × SB05.10

disrupts the reading frame for the C-terminal portion of the protein.

Transformation: Transformation was performed as described previously (OSMANI *et al.* 1987) with the exception that the lytic solution contained 1 mg/ml Novozyme 234 (lot PPM3944, InterSpex Products, Inc., Foster City, CA), which was not precipitated with ammonium sulfate. Also, 0.25% β-glucuronidase (Sigma Chemical Co.) and 10 mg/ml BSA (fraction V, Boehringer Mannheim Biochemicals) were added to the lytic solution. Transformed protoplasts were plated in YAG + 0.6 M KCl solid medium. Cotransformation experiments for Table 2 were done with equimolar amounts of the two DNAs, 0.18 pmol.

DAPI staining and immunofluorescence: Conidia were inoculated into liquid YAG medium at a density of 10^4–10^5 spores/ml in petri dishes containing sterile coverslips. The coverslips with adherent germlings were removed after 66 hr of growth at 18°, 8 hr at 32°, or 7.5 hr at 43°. For DAPI staining of nuclei, germlings were fixed and stained for 15 min in a solution of 50 mM potassium phosphate, pH 6.6, 0.2% Triton X-100, 5% glutaraldehyde, and 0.25 μg/ml DAPI (4,6-diamidino-2-phenylindole), and then washed several times in distilled water. Immunofluorescence staining was performed as described previously (OAKLEY *et al.* 1990), with the following modifications (C. ROGHI and N. R. MORRIS, unpublished results). Cell wall digestion was in a solution of 50% v/v egg white, 2 mM EGTA, 2.5% driselase (Sigma Chemical Co.), 1% *Trichoderma harzianum* lysing enzymes (a crude preparation of novozyme used without ammonium sulfate precipitation, Sigma Chemical Co.), and a cocktail of protease inhibitors (10 μg/ml aprotinin, 15.7 μg/ml benzamidine, 10 μg/ml leupeptin, 10 μg/ml pepstatin, 17.4 μg/ml phenylmethylsulfonyl fluoride, 0.1 mg/ml soybean trypsin inhibitor, 10 μg/ml Nα-p-tosyl-L-arginine methyl ester, and 10 μg/ml N-tosyl-L-phenylalanine chloromethyl ketone). The protease inhibitors greatly improved microtubule staining (C. ROGHI and N. R. MORRIS, unpublished results). A digestion time of about 75 min was optimal for microtubule staining. Coverslips were extracted in a solution of 50 mM PIPES, pH 6.7, 25 mM EGTA, 5 mM $MgSO_4$, 10% DMSO, 0.2% NP-40 for 1 min. Incubation with primary antibody was at 28° for 1 hr with mouse anti-alpha-tubulin monoclonal antibody DM 1A (Sigma Chemical Co.) diluted 1:500 in PEM + 3% BSA. Incubation with secondary antibody was at 28° for 1 hr in the dark with goat anti-mouse-IgG conjugated to CY3 (Jackson ImmunoResearch Laboratories) diluted 1:500 in PEM + 3% BSA. Slides were photographed on a Zeiss Axioplan microscope with a 100× Neofluar objective and TMax ASA 100 or 400 film (Kodak).

RESULTS

The *snfA890* mutation confers sensitivity to cold and benomyl: Following UV mutagenesis, we identified 1000 revertants of the *nudF6* heat-sensitive growth phenotype. The revertants were screened for the presence of extragenic suppressors (as described below). They were also screened for the presence of a conditional-lethal phenotype (sensitivity to cold, DMSO, or salt) to facilitate future cloning of the suppressor genes. This article focuses on one extragenic suppressor mutation, designated *snfA890* for suppressor of *nudF*, which also

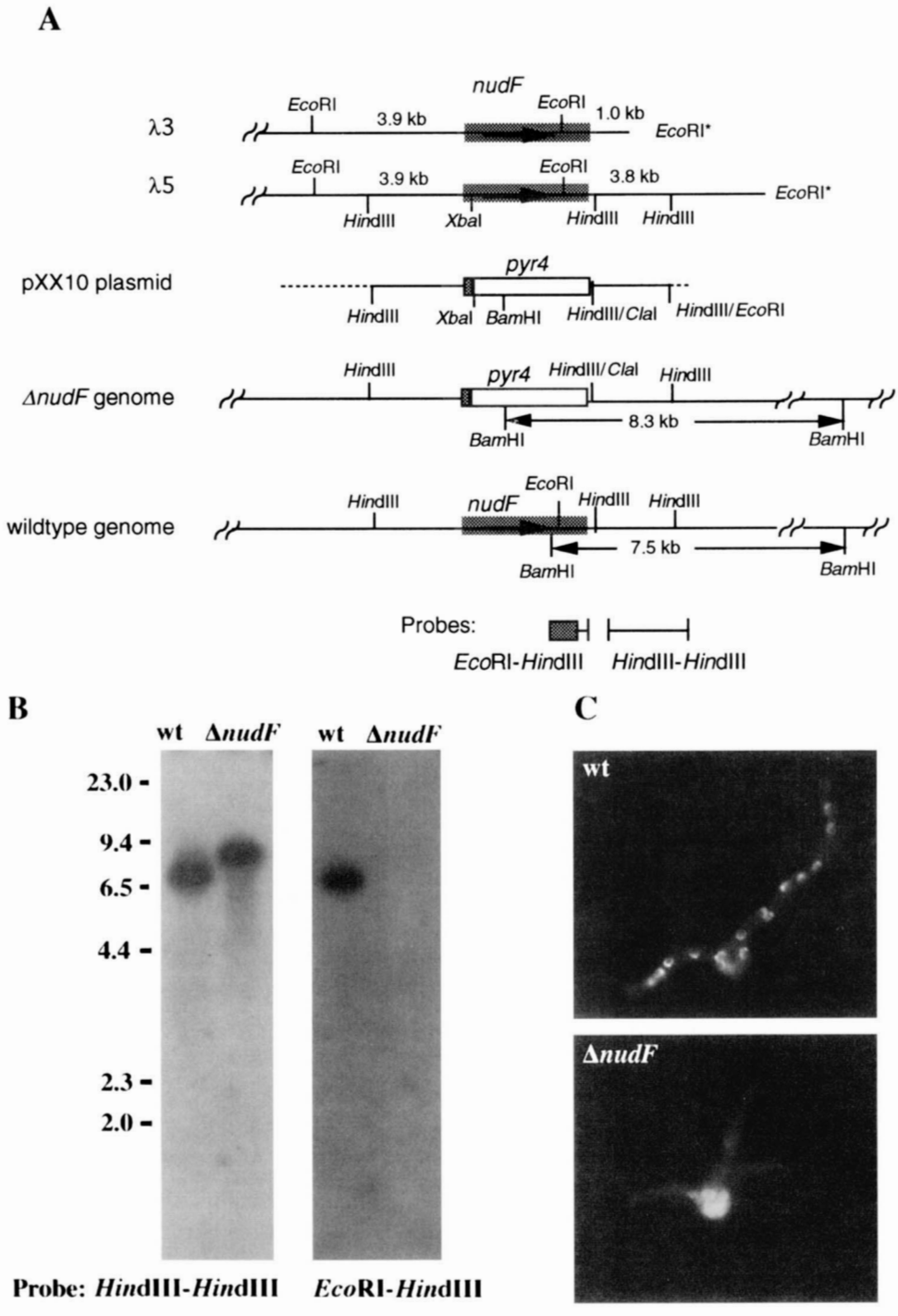

FIGURE 1.—Construction of Δ*nudF* strain ΔF54. (A) Diagram depicting relevant *nudF* clones and the *nudF* region of the genome in Δ*nudF* and wild-type strains. The λ3 and λ5 genomic clones were used in constructing plasmid pXX10. The Δ*nudF* strain ΔF54 was generated by integration of linearized pXX10 DNA into the wild-type genomic *nudF* locus. Thin black lines represent genomic DNA, dotted lines indicate vector DNA, and double wavy lines are breaks in the DNA sequence for diagrammatic purposes. The shaded box represents the *nudF* coding sequence (the arrow indicates the direction of transcription), and the white box represents the *pyr4* coding sequence. Restriction sites used for cloning and the *Bam*HI sites and probes used for Southern blotting are indicated. (B) Southern blotting to verify that Δ*nudF* has replaced *nudF* in strain ΔF54. Genomic DNA from Δ*nudF* strain ΔF54 or wild-type strain R153 was digested with *Bam*HI, transferred to a membrane, and probed with a *nudF* flanking probe (*Hin*dIII-*Hin*dIII) or an internal *nudF* probe (*Eco*RI-*Hin*dIII). Sizes of marker DNA fragments are indicated on the left, in kb. (C) The nuclear migration defect of ΔF54. DAPI staining to visualize nuclei of GR5 (wild type) and ΔF54 (Δ*nudF*) germlings grown at 43°.

confers cold-sensitivity. The remaining suppressors will be described elsewhere.

At restrictive temperature for *nudF6* (43°), *nudF6 snfA890* strains produced colonies intermediate in size between wild-type colonies and the minute hs^- *nudF6* colonies (Figure 2A). We showed that the *nudF6 snfA890* strain DW15 carried an extragenic suppressor by crossing it to $nudF^+$ $snfA890^+$ strain R153. About 25% of the progeny had a heat-sensitive recombinant phenotype (*i.e.*, were $nudF^-$ $snfA^+$), indicating that the suppressor mutation was unlinked to *nudF*. *nudF6 snfA890* strains are sensitive to cold (18°) and to the microtubule-destabilizing drug benomyl at concentrations of 0.2 μg/ml and higher (Figures 2A, B).

Progeny of the DW15 (*nudF6 snfA890*) × R153 cross were analyzed to determine whether the *nudF* suppressor mutation (*snfA890*) was also responsible for the observed cold-sensitivity (cs^-) and benomyl-sensitivity (ben^s). If the *snfA890* suppressor mutation also caused cold-sensitivity and benomyl-sensitivity, one would not expect to find any recombinant hs^- cs^- (*i.e.*, $nudF^-$ $snfA^+$ cs^-) or hs^- ben^s progeny. Of 200–400 progeny

TABLE 2

Wild-type *tubA* DNA repairs the cold-sensitivity of *snfA890*

Recipient strain	Relevant genotype	Transforming DNA	Total no. of transformants	No. of cs^+ transformants
DW26	*snfA890, pyrG89*	$pyrG^+$	200	0
		$pyrG^+$, lin. pDW1	245	59
DW29	*tubA1, pyrG89*	$pyrG^+$	200	0
		$pyrG^+$, lin. pDW1	200	30

A. nidulans protoplasts were incubated with DNA in a cotransformation experiment. $pyrG^+$ plasmid DNA (circular) provided a selectable marker. The second plasmid, linearized pDW1, contained only the coding sequence of *tubA* (with no promoter).

tested in different experiments, none exhibited the hs^- cs^- or hs^- ben^s phenotypes. Similarly, all cs^- progeny were also ben^s. Thus, the mutations causing cold- and benomyl-sensitivity are tightly linked to the *snfA890* suppressor mutation and to each other. Presumably, the same mutation causes all three phenotypes (suppression of *nudF6*, cold-sensitivity, and benomyl-sensitivity).

About 25% of the progeny from the DW15 (*nudF6 snfA890*) × R153 cross generated colonies that were larger at 43° than the intermediate-sized *nudF6 snfA890* colonies and slightly smaller than wild-type colonies (Figure 2A). This class did not sporulate (conidiate) as well as the wild type at 43°. These progeny were also sensitive to cold and benomyl (Figure 2, A and B), suggesting that they might carry *snfA890* without *nudF6*. This was verified by crosses of 3 putative $nudF^+$ *snfA890* progeny to a $nudF^-$ strain, each of which yielded about 25% hs^- progeny.

To test whether *snfA890* is dominant or recessive, diploids were constructed between *snfA890* and $snfA^+$ strains. Heterozygous *snfA890*/$snfA^+$ strains were cs^+ compared to homozygous controls at 18° (Figure 2C), indicating that the cs^- phenotype associated with *snfA890* is recessive. By contrast, the benomyl-sensitive phenotype appeared to be semidominant. We were unable to make diploid strains homozygous for *nudF6* and heterozygous for *snfA*. Therefore, we could not determine whether the suppressor phenotype itself is recessive or dominant.

The *snfA890* mutation is in the *tubA* gene: The *snfA890* mutation was mapped to chromosome *VIII* by standard parasexual genetic methods (CLUTTERBUCK 1974; TIMBERLAKE and MARSHALL 1988). A diploid was constructed between strains DW15 (*snfA890*) and FGSC154 ($snfA^+$), which has marker mutations on each *A. nidulans* chromosome. The diploid was treated with benomyl to produce haploid sectors and the chromosomal location of *snfA890* determined by its segregation

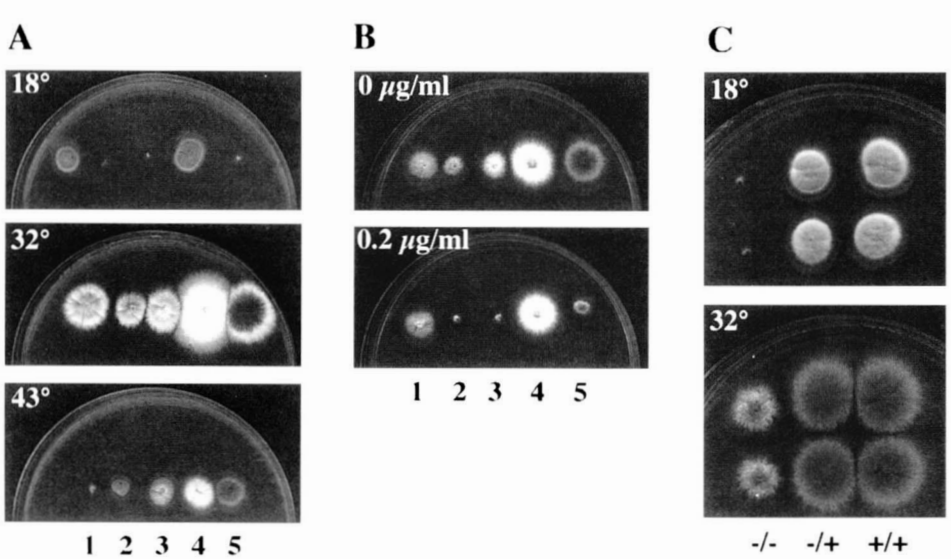

FIGURE 2.—The *snfA890* mutation suppresses the growth defect of *nudF6* and confers sensitivity to cold and benomyl. (A) Growth of *nudF6* and *snfA890* strains at 18°, 32°, and 43°. Strains used were: (1) DW7 (*nudF6*), (2) DW16 (*nudF6 snfA890*), (3) DW17 (*snfA890*), (4) R153 ($nudF^+$ $snfA^+$), and (5) LO12 (*tubA1*). Strains 1 through 4 form an isogenic set. The $nudF^+$ *snfA890* strain exhibited a slight growth defect at 43° and did not sporulate as well as wild type (as seen here by the lack of white spore color). (B) Growth of *nudF6* and *snfA890* strains at 32° on benomyl plates. Strains used are as in part A. (C) The cold sensitivity associated with *snfA890* is recessive. Diploids heterozygous for *snfA890* (−/+) were compared with homozygous *snfA890* (−/−) and homozygous $snfA^+$ diploids (+/+) for growth at 18° and 32°. Strains used were: DW15 / FGSC154 and DW17 / R21 (−/+), two independent isolates of DW15 / DW17 (−/−), and XX20 / R153 and R153 / R21 (+/+).

from the marker mutations. This method suggested that the mutation mapped to chromosome *VIII*. This location was confirmed by conventional mapping with sexual crosses, which demonstrated that *snfA* was loosely linked to the *chaA* gene on chromosome *VIII*.

Several genes in this region of chromosome *VIII* affect nuclear migration, including *nudA*, *nudG*, and *tubA* (which encodes the major alpha tubulin of *A. nidulans*) (DOSHI *et al.* 1991; XIANG *et al.* 1994) (S. BECKWITH and N. R. MORRIS, unpublished results). We determined by crosses that *snfA* was not tightly linked to *nudA* or *nudG* but was very tightly linked to *tubA*. DW17 (*nudF*$^+$ *snfA890*) was crossed to *tubA1* strain LO14. Both *snfA890* and *tubA1* mutations confer sensitivity to cold and benomyl, so recovery of any substantial number of cs$^+$ ben$^+$ recombinant progeny would indicate that these mutations are in different genes. Of 600 progeny analyzed, none were cs$^+$ ben$^+$. Tight linkage between the *snfA890* and *tubA1* mutations in addition to the similar phenotypes of the two mutations suggested that *snfA890* might in fact be an allele of *tubA*.

To test whether the cold sensitivity associated with *snfA890* is due to a mutation in *tubA*, we used DNA-mediated transformation to introduce wild-type genomic *tubA* DNA into *A. nidulans* strain DW26 (*nudF6 snfA890 pyrG89*) and a control strain DW29 (*tubA1 pyrG89*). The strains were cotransformed with linearized plasmid pDW1 (which contains only a promoterless *tubA* coding sequence) and a circular plasmid carrying the *pyrG*$^+$ selectable marker. Integration of linearized *tubA*$^+$ DNA presumably would occur by a double crossover event at the *tubA* locus, generating a transformant with one wild-type copy of *tubA*. When DW26 and DW29 were transformed with the *pyrG*$^+$ plasmid alone, none of the pyr$^+$ transformants were cs$^+$. However, when DW26 and DW29 were transformed with a mixture of the *pyrG*$^+$ plasmid and linearized pDW1 (*tubA*$^+$), many pyr$^+$ transformants were cs$^+$ (Table 2). This indicated that the cs$^-$ phenotype of *snfA890* is caused by a mutation in *tubA*.

To determine directly whether suppression of *nudF6* by *snfA890* is caused by a mutation in *tubA*, we made use of the fact that recipient strain DW26 carries both *nudF6* and *snfA890* mutations (*i.e.*, is hs$^+$). If the *snfA890* suppressor mutation were in *tubA*, pyr$^+$ DW26 transformants with site-specific integration of linearized pDW1 DNA should be hs$^-$ (*i.e., nudF6 snfA*$^+$). One pyr$^+$ DW26 transformant was identified which by Southern blotting showed integration only at the *tubA* locus. This transformant was hs$^-$ and also cs$^+$ ben$^+$. DAPI staining showed that it had a nuclear migration defect. This result showed that the *snfA890* suppressor mutation is in *tubA*, and henceforth the *snfA890* mutation will be designated *tubA22*. Taken together with the linkage data, these data indicate that the *tubA22* mutation causes all three phenotypes observed (suppression of *nudF6*, cold-sensitivity, and benomyl-sensitivity).

Effect of the *tubA22* mutation on nuclear migration and on microtubules: Strains carrying the *tubA22* mutation were examined cytologically for defects in nuclear migration and microtubule stability. To investigate *tubA22* suppression of the *nudF6* nuclear migration defect, germlings grown at restrictive temperature (43°) were stained with DAPI. Nuclei of *nudF6* germlings grown at 43° failed to move from the spore end of the germ tube into the hyphae, in contrast to wild-type nuclei, which were distributed throughout the hyphae (Figure 3). Most *nudF6 tubA22* germlings displayed an intermediate phenotype, with nuclei not distributed as evenly as in the wild type (Figures 3 and 4). Strains carrying *tubA22* alone or *tubA1* showed no nuclear migration defect.

Next, we tested whether the *tubA22* mutation itself might affect nuclear migration at the restrictive temperature for cold-sensitivity (18°). Many *tubA22* germlings (*nudF*$^+$ *or nudF6*) showed an abnormal phenotype at 18°, with small, unevenly distributed DAPI-staining particles (Figure 5). These particles appeared to be condensed or fragmented nuclei but could also represent mitochondrial DNA. Some *tubA1* germlings grown at 18° also showed this phenotype. By contrast, nuclei of *nudF6* and wild-type germlings were evenly distributed along the hyphae at 18°.

Because other *tubA* mutations that are cs$^-$ and ben^s were previously reported to have defects in microtubule stability (GAMBINO *et al.* 1984), *tubA22* germlings were examined for defects in microtubule stability. *nudF*$^+$ *tubA22* germlings grown at 32° did not exhibit a nuclear migration defect or an unusual DAPI staining pattern. However, when stained for tubulin they showed poor microtubule preservation and a low abundance of long cytoplasmic microtubules compared to wild-type germlings (Figure 6). A similar difference in tubulin staining was seen between *tubA22* and wild-type germlings grown at 43°. Decreased stability of microtubules could account for *tubA22* suppression of *nudF6*.

***tubA22* suppresses *nudA*, *nudC*, *nudF*, and *nudG* nuclear migration mutations:** While mapping the *tubA22* mutation, we crossed it to the *nudA* and *nudG* mutations and found that *tubA22* also suppressed these *nud* mutations. Progeny from crosses of DW17 (*nudF*$^+$ *tubA22*) to *nudA1* strain XX3 showed typical *nudA1*, *tubA22*, and wild-type phenotypes at 43°. But 25% of the progeny were intermediate in size between the minute *nudA1* colonies and the large *tubA22* or wild-type colonies (Figure 7). The intermediate-sized colonies at 43° were all cs$^-$, indicating the presence of the *tubA22* mutation and suggesting that this class of progeny represented *nudA1 tubA22* double mutants. Similar results were seen from DW17 (*nudF*$^+$ *tubA22*) crosses to *nudC3*, *nudF7*, and *nudG8* mutants (strains YH1, XX21, and SB05.10) (Figure 7). The presence of the *nud* mutations was verified in each case by crossing two cs$^-$ progeny that were intermediate-sized at 43° to strains carrying the original *nud*

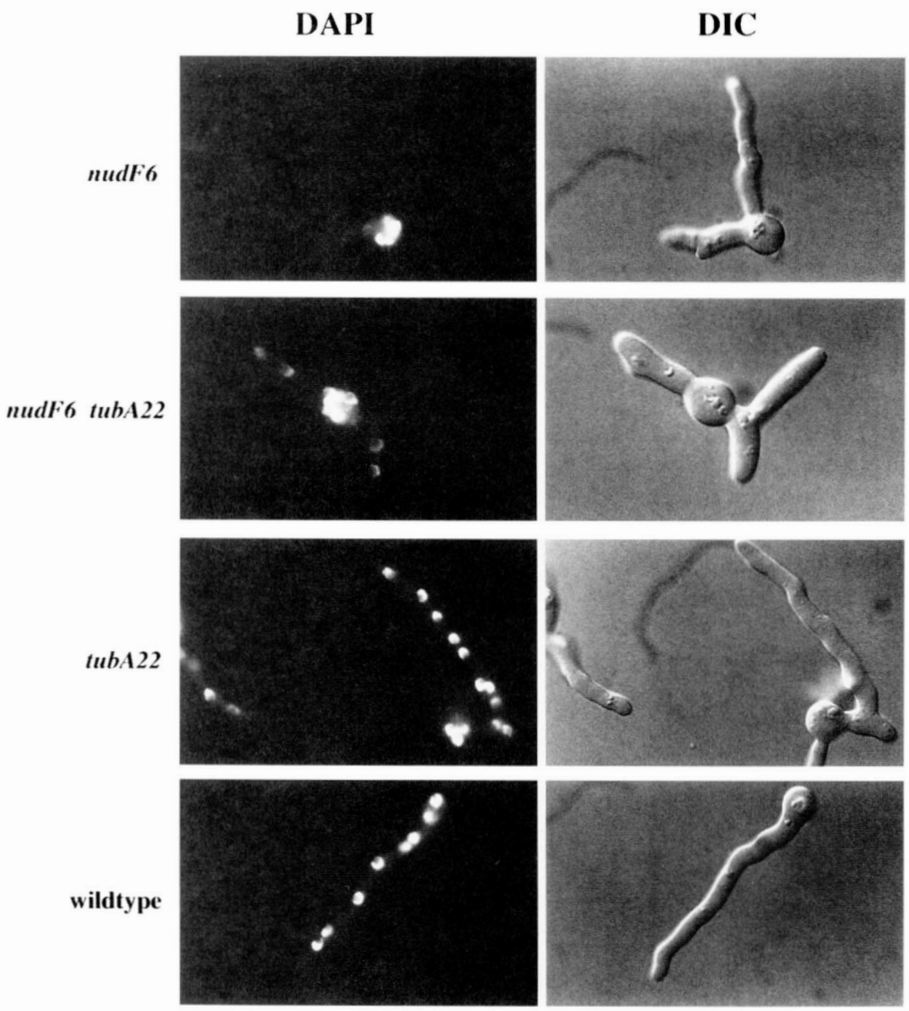

FIGURE 3.—*tubA22* suppresses the nuclear migration defect of *nudF6* at 43°. Spores from isogenic strains with the indicated genotypes (DW7, DW16, DW17, and R153) were germinated and grown at 43°. The panels on the left show nuclei stained with DAPI, and the panels on the right show the DIC (differential interference contrast) view of same field.

mutation or to a wild-type strain. These crosses yielded, respectively, approximately equal numbers of hs^- (*nud*) and intermediate-sized progeny at 43° or approximately equal numbers of all four size classes at 43°. *tubA22* therefore suppressed the growth defect caused by the *nudA1, nudC3, nudF6, nudF7,* and *nudG8* mutants.

To determine if *tubA22* acts as a bypass suppressor, it was crossed to strains that made no active *nudF* or *nudA* product. Strain DW27 (*nudF*$^+$ *tubA22 pyrG89*) was crossed to strain ΔF54 (Δ*nudF*) or XX60 (Δ*nudA*). The *nudF* coding sequence is deleted in ΔF54, except for 12 N-terminal amino acids (Figure 1; MATERIALS AND METHODS). XX60 carries a deletion/disruption of *nudA* that removes more than half of the coding sequence and should inactivate the dynein motor (XIANG *et al.* 1995b). Both strains produce minute colonies (Figure 8, upper panel), and both have a nuclear migration defect at 43° and 32° (Figure 1C shows the defect for Δ*nudF* strain ΔF54 and XX60 is similar). In addition, the deleted sequence in each case was replaced with a pyr$^+$ marker. Because both parents of the cross carried the *pyrG89* mutation at the *pyrG* locus, progeny carrying Δ*nudF* or Δ*nudA* could be identified by their ability to grow on medium lacking uridine and uracil.

Strain	Relevant genotype	No. of germlings	% nud	% intermed.	% wt
DW7	*nudF6*	100	95	5	0
DW16	*nudF6, tubA22*	100	31	69	0
XX3	*nudA1*	100	85	15	0
DW30	*nudA1, tubA22*	105	42	58	0

FIGURE 4.—*tubA22* suppression of *nud* nuclear migration defects. Germlings grown at 43° were stained with DAPI and their nuclear migration phenotypes scored as nud if one or no nuclei entered the germ tube, as intermediate if more than one nucleus entered the germ tube but nuclei were not evenly distributed, and as wild type if the nuclei in the germ tube were evenly distributed.

About 25% of the progeny from crosses of DW27 (*tubA22*) to ΔF54 (Δ*nudF*) or XX60 (Δ*nudA*) were intermediate in size at 43°, suggesting that *tubA22* suppressed the growth defect of these *nud* mutants as well. The genotype of the putative double mutants was verified by their cold-sensitivity (for *tubA22*) and their ability to grow without uridine and uracil (for the Δ*nud* mutations).

Finally, DAPI staining of *nudF6 tubA22* and *nudA1*

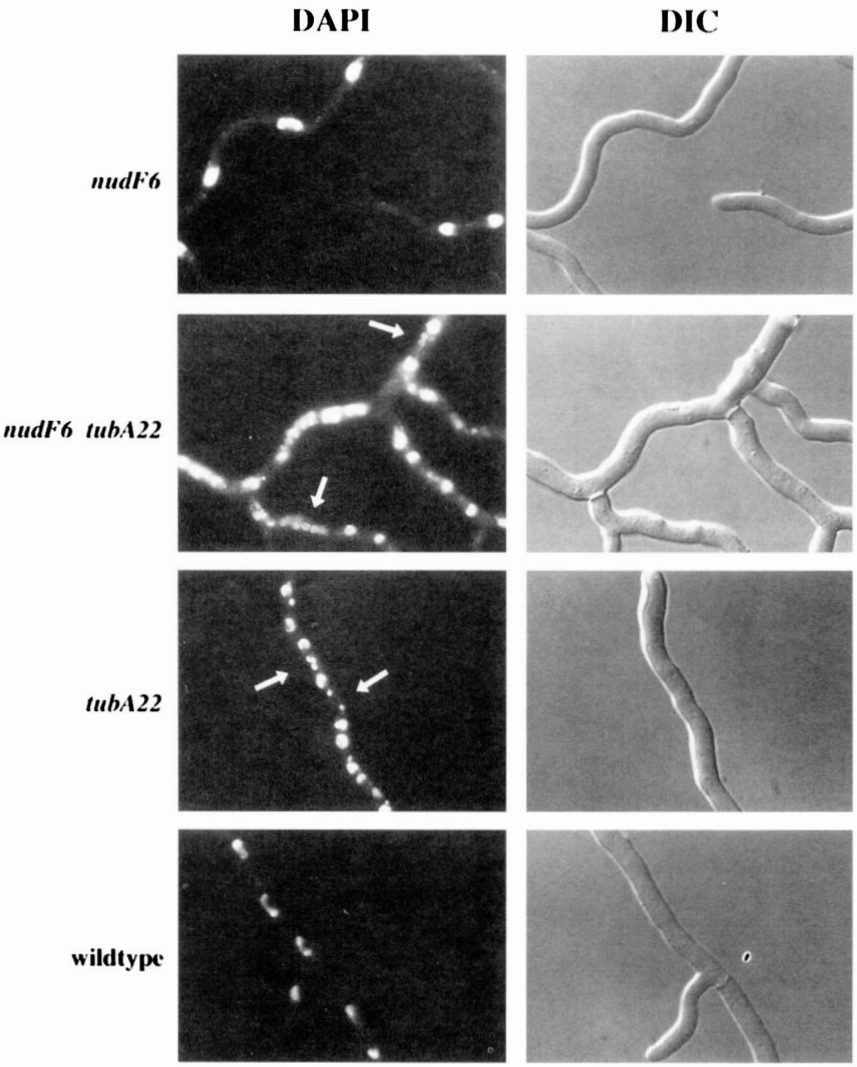

FIGURE 5.—*tubA22* germlings have an unusual DAPI staining pattern at 18°. Spores from isogenic strains with the indicated genotypes (DW7, DW16, DW17, and R153) were germinated and grown at 18°, then stained with DAPI. Left and right panels show DAPI and DIC views, respectively, of the same field. Arrows indicate small, unevenly distributed DAPI-staining structures.

tubA22 double mutant germlings grown at 43° (Figures 3 and 4) showed that *tubA22* suppression of the *nudF* and *nudA* growth defects correlated with suppression of the nuclear migration defect. Half or more of the *nud tubA22* germlings showed an intermediate phenotype, with nuclei migrating into the hyphae but not as

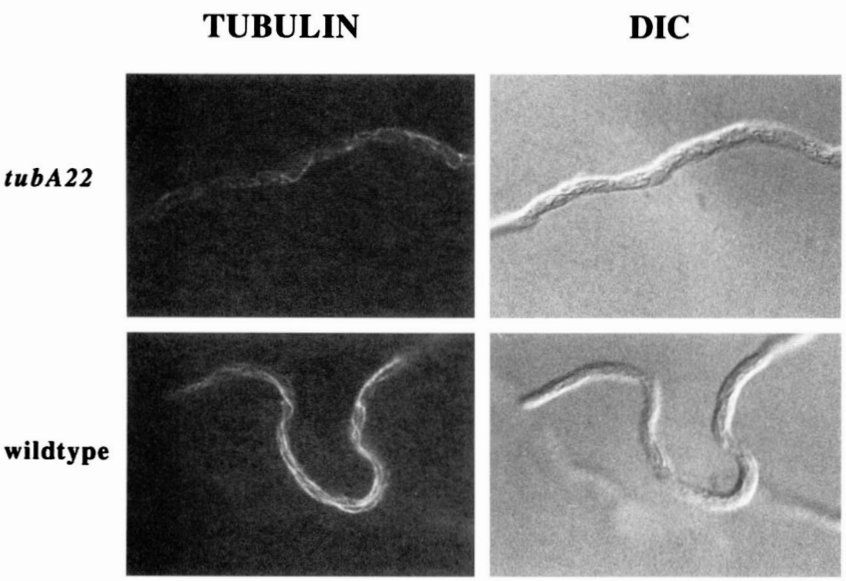

FIGURE 6.—*tubA22* alters microtubule staining. Germlings from isogenic *tubA22* and wild-type strains (DW17 and R153) were grown at 32°, fixed, and stained with anti-tubulin antibody (left panel). The right panel shows the DIC view of the same field.

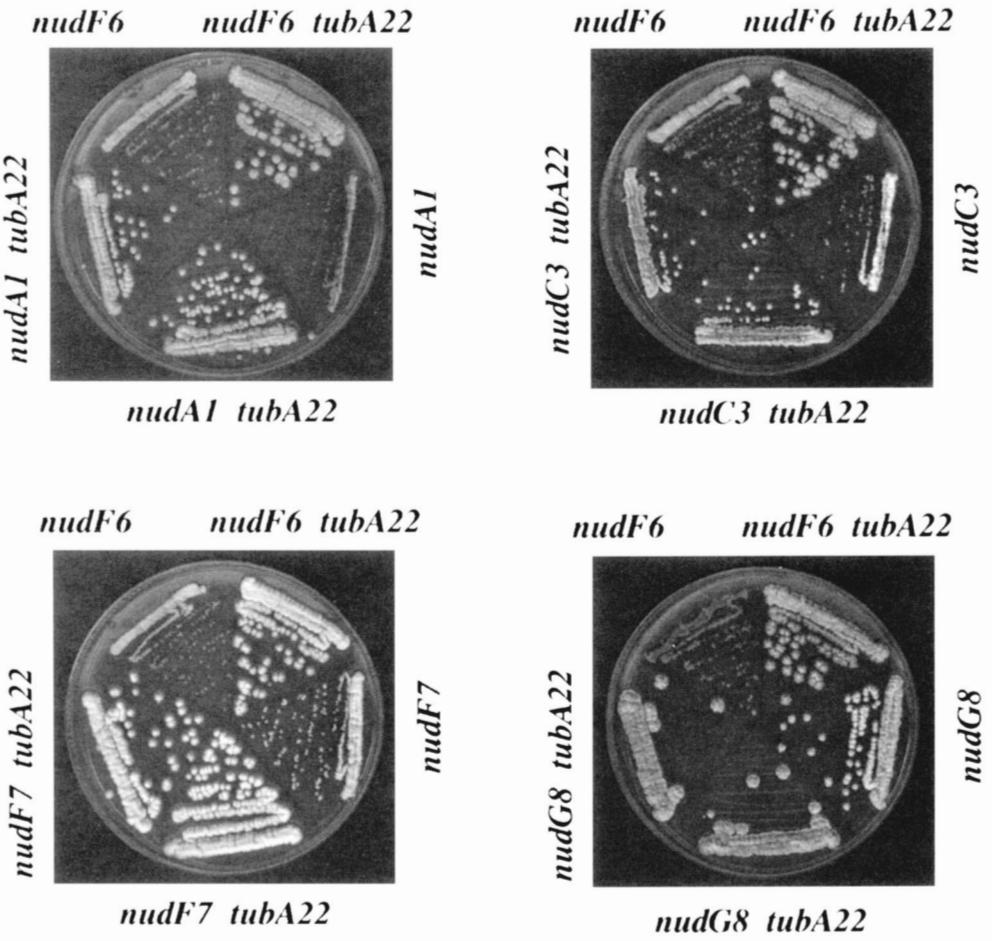

FIGURE 7.—*tubA22* suppresses the growth defect caused by *nudA, nudC, nudF,* and *nudG* hs⁻ mutants. Double mutants carrying a *nud* mutation and *tubA22* were streaked to single colony and grown at 43°. Compare each *nud* mutant with the corresponding *nud tubA22* double mutant (two independent isolates) within the same panel. On each plate, the *nudF6* strain DW7 and *nudF6 tubA22* strain DW16 are shown for comparison. Strains used were: XX3 (*nudA1*), DW30 and DW31 (*nudA1 tubA22*), YH1 (*nudC3*), DW32 (*nudC3 tubA22*), XX21 (*nudF7*), DW33 (*nudF7 tubA22*), SB05.10 (*nudG8*), and DW34 (*nudG8 tubA22*). Each *nud tubA22* double mutant is isogenic or nearly isogenic with its *nud* parent.

evenly distributed as in the wild type (Figure 4). By contrast, most germlings from the *nud* parent had a nud phenotype. Presumably *tubA22* also suppresses the growth defect of the *nudC* and *nudG* mutants by suppressing the nuclear migration defect.

Benomyl suppresses the nuclear migration mutations: The *tubA22* mutation suppressed the *nud* mutations and apparently destabilized microtubules. We wanted to determine whether suppression of the *nud* mutations specifically required the *tubA22* mutation or whether it could be accomplished by other means of microtubule destabilization. Therefore, we tested the ability of the microtubule-destabilizing agent benomyl to suppress the *nud* mutations. The *nud* mutants described previously (*nudA1, ΔnudA, nudF6, nudF7, ΔnudF, nudC3, nudG8*) were streaked on rich medium plates containing different concentrations of benomyl and incubated at 43°. The growth defect of all of the *nud* mutations was suppressed by 0.5 μg/ml benomyl (Figure 8). This low concentration of benomyl prevented sporulation (conidiation) of the wild-type strain but did not affect its colony size. Low concentrations of benomyl had only a minor effect compared to *tubA22* in improving nuclear migration at early times after germination. However, it is likely that benomyl suppresses the growth defect of the *nud* mutants by suppressing the nuclear migration defect.

DISCUSSION

Here we report the characterization of an extragenic suppressor of the *nudF6* nuclear migration mutation, initially designated *snfA890* for suppressor of *nudF*. The suppressor mutation confers sensitivity to cold and benomyl, two treatments that destabilize microtubules. We determined that the *snfA890* mutation is an allele of *tubA*, which encodes the major *A. nidulans* alpha tubulin (DOSHI *et al.* 1991) (henceforth the mutation will be called *tubA22*). It was previously suggested that the *tubA1* and *tubA4* mutations confer sensitivity to cold and benomyl because they destabilize microtubules, such that additional microtubule destabilization by cold

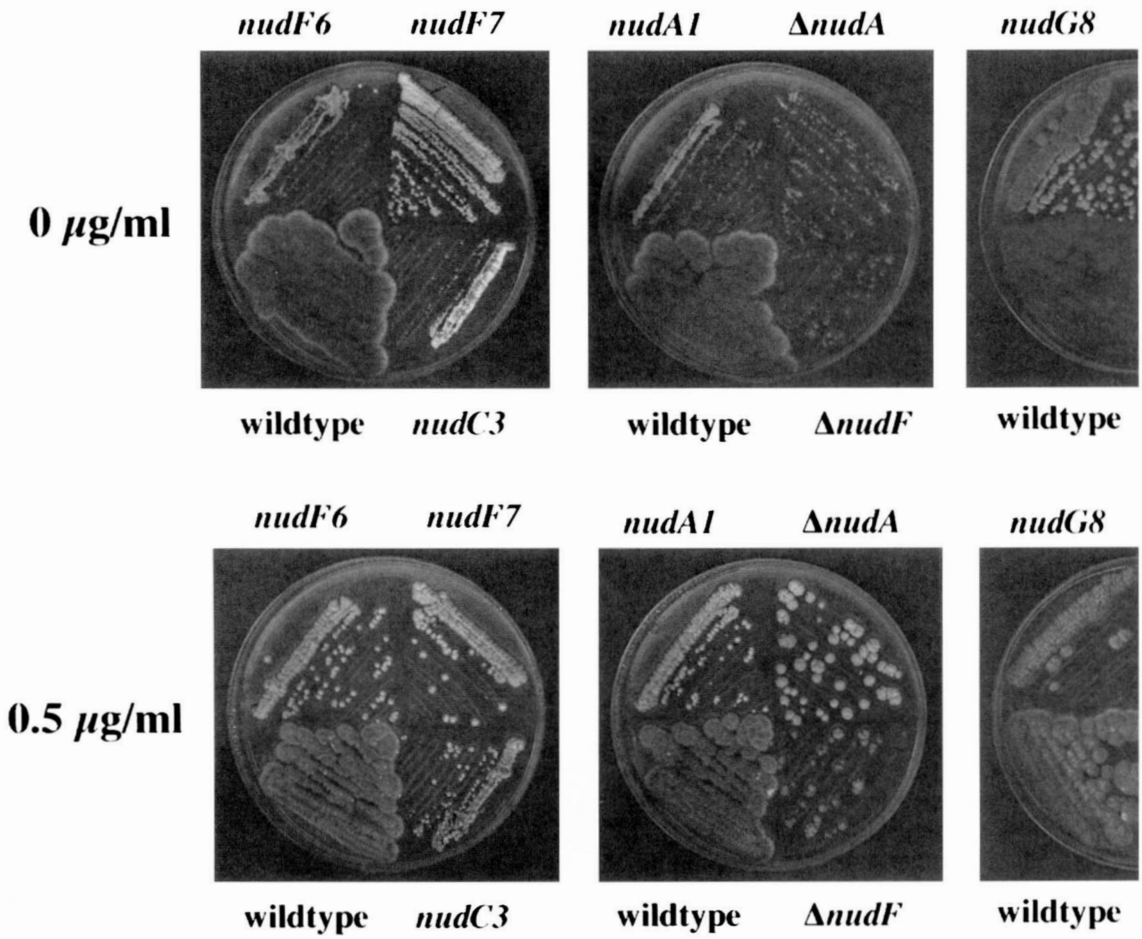

FIGURE 8.—Benomyl suppresses the growth defect of the *nud* mutants. *nudA*, *nudC*, *nudF*, and *nudG* mutants were streaked to single colony and grown at 43° in the absence (upper panel) or presence (lower panel) of the microtubule-destabilizing drug benomyl. Strains used were: XX20 (*nudF6*), XX21 (*nudF7*), YH1 (*nudC3*), XX3 (*nudA1*), XX60 (Δ*nudA*), ΔF54 (Δ*nudF*), SB05.10 (*nudG8*), and SJ002 for a wild-type control.

or benomyl severely reduces growth (OAKLEY and MORRIS 1981; OAKLEY *et al.* 1987a; GAMBINO *et al.* 1984). The cold- and benomyl-sensitivity of *tubA22* mutants and their alteration in microtubule staining are consistent with a defect in microtubule stability.

The *tubA22* mutation also suppresses the growth defect of *nudA*, *nudC*, and *nudG* mutations. Suppression of the *nudF6* and *nudA1* growth defect correlates with improved nuclear migration, and we predict that this is also the case for the other *nud* mutants. The *tubA22* mutation suppresses several different mutations in *nudA* and *nudF*, including the Δ*nudA* and Δ*nudF* deletions, which give no full-length protein product. Our data therefore suggest that the *tubA22* mutation is a bypass suppressor of *nudA* and *nudF* mutations rather than an allele-specific suppressor.

Finally, we showed that the *tubA22* mutation is not specifically required to suppress the *nud* mutants, because destabilization of microtubules by the drug benomyl had the same effect (in the absence of the *tubA22* mutation). This indicated that destabilization of microtubules in general would suppress the *nud* mutations.

Suppression of the *nud* growth defect is particularly interesting in the case of the *nudA1* and Δ*nudA* mutants, which carry mutations in the cytoplasmic dynein heavy chain. Dynein, a microtubule motor with ATPase activity, is required for nuclear migration in *A. nidulans* (XIANG *et al.* 1994). The *nudA1* mutant produces very little or no detectable dynein heavy chain at the restrictive temperature, and the Δ*nudA* strain produces little or no truncated product, which is presumably inactive (XIANG *et al.* 1995b). Together, the results of the *tubA22* and benomyl suppression tests suggest that nuclei can move in the absence of active cytoplasmic dynein motor if microtubules are destabilized.

We propose three models to explain how microtubule destabilization might improve nuclear movement in the absence of active dynein. First, destabilization could allow passive, microtubule-independent movement by removing microtubules interfering with the free movement of nuclei. We do not think this likely. Second, microtubule depolymerization itself (shortening or increased treadmilling of microtubules) could accomplish nuclear movement in the absence of motor proteins. For example, cytoplasmic microtubules may connect nuclei to the hyphal tip or another anchoring

site (MORRIS *et al.* 1995), and shortening of such microtubules would allow movement of the nucleus. Microtubule shortening and treadmilling have been proposed to move chromosomes during mitosis, and there is evidence to support these ideas (INOUÉ 1981; KOSHLAND *et al.* 1988; MITCHISON 1988; COUE *et al.* 1991). Third, microtubule destabilization could allow another motor protein to substitute for dynein, such as *klpA*, the *A. nidulans* equivalent of the KAR3 kinesin-related protein, which has the same polarity of movement along microtubules as dynein (O'CONNELL *et al.* 1993; ENDOW *et al.* 1994). The second and third models may be related, because motor proteins themselves can stimulate microtubule depolymerization and couple microtubule depolymerization to chromosome movement (ENDOW *et al.* 1994; DESAI and MITCHISON 1995; LOMBILLO *et al.* 1995a,b).

Suppression of the other *nud* mutations by *tubA22* or benomyl can be explained by the same models. The *nudA*, *nudC*, and *nudF* mutants at their restrictive temperature do not show any obvious defect in cytoplasmic or astral microtubules (OSMANI *et al.* 1990) (C. ANDRADE-MONTEIRO and N. R. MORRIS, unpublished results). The *nudC*, *nudF*, and *nudG* products are likely to act at intermediate steps in activating dynein or another motor protein. If so, these mutants would be suppressed by the same conditions that suppressed the dynein mutants.

In summary, we have found that nuclear migration mutations in *nudA*, *nudC*, *nudF*, and *nudG* can be suppressed by a tubulin mutation or by treatment with benomyl, both of which destabilize microtubules. In particular, our results with *nudA* mutants suggest that microtubule destabilization allows nuclear migration to proceed even in the absence of cytoplasmic dynein.

We would like to thank our colleague Dr. HERBERT GELLER for the use of his microscope and DR. CHRISTIAN ROGHI, DR. SUSAN BECKWITH, DR. GUSTAVO GOLDMAN, and YA-HUI CHIU from the MORRIS laboratory for stimulating discussion. This work was supported by National Institutes of Health grants GM29228 and GM34711 to N.R.M.

LITERATURE CITED

BARTH, P. G., 1987 Disorders of neuronal migration. Can. J. Neurol. Sci. **14**: 1–16.

BOOK, K. J., R. HOWARD and D. K. MOREST, 1991 Direct observation *in vitro* of how neuroblasts migrate: Medulla and cochleovestibular ganglion of the chick embryo. Exp. Neurol. **111**: 228–243.

CLUTTERBUCK, A. J., 1974 *Aspergillus nidulans*, pp. 447–510 in *Handbook of Genetics*, Vol.1, edited by R. C. KING. Plenum Press, New York.

COUE, M., V. A. LOMBILLO and J. R. MCINTOSH, 1991 Microtubule depolymerization promotes particle and chromosome movement *in vitro*. J. Cell Biol. **112**: 1165–1175.

DAN, K., 1979 Studies on unequal cleavage in sea urchins I. Migration of the nuclei to the vegetal pole. Devel. Growth and Differ. **21**: 527–535.

DESAI, A., and T. J. MITCHISON, 1995 A new role for motor proteins as couplers to depolymerizing microtubules. J. Cell Biol. **128**: 1–4.

DOSHI, P., C. A. BOSSIE, J. H. DOONAN, G. S. MAY and N. R. MORRIS, 1991 Two α-tubulin genes of *Aspergillus nidulans* encode divergent proteins. Mol. Gen. Genet. **225**: 129–141.

ENDOW, S. A., S. J. KANG, L. L. SATTERWHITE, M. D. ROSE, V. P. SKEEN *et al.*, 1994 Yeast Kar3 is a minus-end microtubule motor protein that destabilizes microtubules preferentially at the minus ends. EMBO J. **13**: 2708–2713.

ESHEL, D., L. A. URRESTARAZU, S. VISSERS, J.-C. JAUNIAUX, J. C. VAN-VLIET-REEDIJK *et al.*, 1993 Cytoplasmic dynein is required for normal nuclear segregation in yeast. Proc. Natl. Acad. Sci. USA **90**: 11172–11176.

GAMBINO, J., L. G. BERGEN and N. R. MORRIS, 1984 Effects of mitotic and tubulin mutations on microtubule architecture in actively growing protoplasts of *Aspergillus nidulans*. J. Cell Biol. **99**: 830–838.

HUFFAKER, T. C., J. H. THOMAS and D. BOTSTEIN, 1988 Diverse effects of β-tubulin mutations on microtubule formation and function. J. Cell Biol. **106**: 1997–2010.

INOUÉ, S., 1981 Cell division and the mitotic spindle. J. Cell Biol. **91**: 131s–147s.

KÄFER, E., 1977 Meiotic and mitotic recombination in *Aspergillus nidulans* and its chromosomal aberrations. Adv. Genet. **19**: 33–131.

KLOMINEK, J., K.-G. SUNDQVIST and K.-H. ROBERT, 1991 Nucleokinesis: Distinct pattern of cell translocation in response to an autocrine motility factor-like substance or fibronectin. Proc. Natl. Acad. Sci. USA **88**: 3902–3906.

KOSHLAND, D. E., T. J. MITCHISON and M. W. KIRSCHNER, 1988 Polewards chromosome movement driven by microtubule depolymerization *in vitro*. Nature **331**: 499–504.

LI, Y.-Y., E. YEH, T. HAYS and K. BLOOM, 1993 Disruption of mitotic spindle orientation in a yeast dynein mutant. Proc. Natl. Acad. Sci. USA **90**: 10096–10100.

LOMBILLO, V. A., C. NISLOW, T. J. YEN, V. I. GELFAND and J. R. MCINTOSH, 1995a Antibodies to the kinesin motor domain and CENP-E inhibit microtubule depolymerization-dependent motion of chromosomes in vitro. J. Cell Biol. **128**: 107–115.

LOMBILLO, V. A., R. J. STEWART and J. R. MCINTOSH, 1995b Minus-end-directed motion of kinesin-coated microspheres driven by microtubule depolymerization. Nature **373**: 161–164.

MITCHISON, T. J., 1988 Microtubule dynamics and kinetochore function in mitosis. Annu. Rev. Cell Biol. **4**: 527–549.

MORRIS, N. R., 1976 Mitotic mutants of *Aspergillus nidulans*. Genet. Res. Camb. **26**: 237–254.

MORRIS, N. R., X. XIANG and S. M. BECKWITH, 1995 Nuclear migration advances in fungi. Trends Cell Biol. **5**: 278–282.

O'CONNELL, M. J., P. B. MELUH, M. D. ROSE and N. R. MORRIS, 1993 Suppression of the *bimC4* mitotic spindle defect by deletion of *klpA*, a gene encoding a KAR3-related kinesin-like protein in *Aspergillus nidulans*. J. Cell Biol. **120**: 153–162.

OAKLEY, B. R., and N. R. MORRIS, 1980 Nuclear movement is β-tubulin-dependent in *Aspergillus nidulans*. Cell **19**: 255–262.

OAKLEY, B. R., and N. R. MORRIS, 1981 A β-tubulin mutation in *Aspergillus nidulans* that blocks microtubule function without blocking assembly. Cell **24**: 837–845.

OAKLEY, B. R., C. E. OAKLEY and J. E. RINEHART, 1987a Conditionally lethal *tubA* α-tubulin mutations in *Aspergillus nidulans*. Mol. Gen. Genet. **208**: 135–144.

OAKLEY, B. R., J. E. RINEHART, B. L. MITCHELL, C. E. OAKLEY, C. CARMONA *et al.*, 1987b Cloning, mapping and molecular analysis of the *pyrG* (orotidine-5′-phosphate decarboxylase) gene of *Aspergillus nidulans*. Gene **61**: 385–399.

OAKLEY, B. R., C. E. OAKLEY, Y. YOON and M. K. JUNG, 1990 γ-Tubulin is a component of the spindle pole body that is essential for microtubule function in *Aspergillus nidulans*. Cell **61**: 1289–1301.

OSMANI, S. A., G. S. MAY and N. R. MORRIS, 1987 Regulation of the mRNA levels of *nimA*, a gene required for the G2-M transition in *Aspergillus nidulans*. J. Cell Biol. **104**: 1495–1504.

OSMANI, A. H., S. A. OSMANI and N. R. MORRIS, 1990 The molecular cloning and identification of a gene product specifically required for nuclear movement in *Aspergillus nidulans*. J. Cell Biol. **111**: 543–551.

PLAMANN, M., P. F. MINKE, J. H. TINSLEY and K. S. BRUNO, 1994 Cytoplasmic dynein and actin-related protein Arp1 are required for normal nuclear distribution in filamentous fungi. J. Cell Biol. **127**: 139–149.

PONTECORVO, G., J. A. ROPER, L. M. HEMMONS, K. D. MACDONALD and A. W. J. BUFTON, 1953 The genetics of *Aspergillus nidulans*. Adv. Genet. **5**: 141–238.

REEVE, W. J. D., and F. P. KELLY, 1983 Nuclear position in the cells of the mouse early embryo. J. Embryol. Exp. Morph. **75**: 117–139.

REINER, O., R. CARROZZO, Y. SHEN, M. WEHNERT, F. FAUSTINELLA *et al.*, 1993 Isolation of a Miller-Dieker lissencephaly gene containing G protein β-subunit-like repeats. Nature **364**: 717–721.

ROBB, M. J., M. A. WILSON and P. J. VIERULA, 1995 A fungal actin-related protein involved in nuclear migration. Mol. Gen. Genet. **247**: 583–590.

ROSE, M. D., 1991 Nuclear fusion in yeast. Annu. Rev. Microbiol. **45**: 539–567.

SAMBROOK, J., E. F. FRITSCH and T. MANIATIS, 1989 *Molecular Cloning, a Laboratory Manual*. Cold Spring Harbor Laboratory Press, Cold Spring Harbor, NY. 2nd ed.

SCHATTEN, G., 1982 Motility during fertilization. Int. Rev. Cytol. **79**: 59–163.

SCHROER, T. A., 1994 New insights into the interaction of cytoplasmic dynein with the actin-related protein, Arp1. J. Cell Biol. **127**: 1–4.

SMITH, J. L., and G. C. SCHOENWOLF, 1988 Role of cell-cycle in regulating neuroepithelial cell shape during bending of the chick neural plate. Cell Tissue Res. **252**: 491–500.

TIMBERLAKE, W. E., and M. A. MARSHALL, 1988 Genetic regulation of development in *Aspergillus nidulans*. Trends Genet. **4**: 162–169.

VALLEE, R., 1993 Molecular analysis of the microtubule motor dynein. Proc. Natl. Acad. Sci. USA **90**: 8769–8772.

XIANG, X., S. M. BECKWITH and N. R. MORRIS, 1994 Cytoplasmic dynein is involved in nuclear migration in *Aspergillus nidulans*. Proc. Natl. Acad. Sci. USA **91**: 2100–2104.

XIANG, X., A. H. OSMANI, S. A. OSMANI, M. XIN and N. R. MORRIS, 1995a *NudF*, a nuclear migration gene in *Aspergillus nidulans*, is similar to the human *LIS-1* gene required for neuronal migration. Molec. Biol. Cell **6**: 297–310.

XIANG, X., C. ROGHI and N. R. MORRIS, 1995b Characterization and localization of the cytoplasmic dynein heavy chain in *Aspergillus nidulans*. Proc. Natl. Acad. Sci. USA, in press.

ZALOKAR, M., and I. ERK, 1976 Division and migration of nuclei during early embryogenesis of *Drosophila melanogaster*. J. Microscopie Biol. Cell. **25**: 97–106.

Communicating editor: P. J. PUKKILA